

Exciton dynamics in solid-state green fluorescent protein

Christof P. Dietrich^{1, a)}, Marie Siegert¹, Simon Betzold¹, Jürgen Ohmer², Utz Fischer², and Sven Höfling^{1,3}

¹*Technische Physik, University of Würzburg, Am Hubland, 97074 Würzburg, Germany*

²*Department of Biochemistry, University of Würzburg, Am Hubland, 97074 Würzburg, Germany and*

³*SUPA, School of Physics and Astronomy, University of St Andrews, North Haugh, KY16 9SS St Andrews, United Kingdom*

(Dated: 9 December 2016)

We study the decay characteristics of Frenkel excitons in solid-state enhanced green fluorescent protein (eGFP) dried from solution. We further monitor the changes of the radiative exciton decay over time by crossing the phase transition from the solved to the solid state. Complex interactions between protonated and deprotonated states in solid-state eGFP can be identified from temperature-dependent and time-resolved fluorescence experiments that further allow the determination of activation energies for each identified process.

Keywords: fluorescent proteins; exciton dynamics; proton transfer

In the last two decades, fluorescent proteins (FPs) have revolutionized many different areas of research. In particular biology, medicine and physiology are probably the uttermost affected. Their sublime photophysical and biochemical properties have created new eras of investigations such as live-cell¹ and super-resolution imaging² and have fundamentally changed research disciplines such as molecular biology and cell biology. FPs are most commonly used as biological markers or fluorescent probes in living organisms. FPs have therein enabled the investigation of nerve cell developments or cancer cell spreadings³. Those seminal advancements are first and foremost related to the ability to express FPs in any possible cell type without affecting intrinsic cell properties which is due to the fact that FP chromophores can be formed by autocatalytic cyclization without the need of a cofactor⁴. Combined with an excellent photophysical stability, FPs have become one of the most important tools in bio-science.

Another interesting development has taken place in recent years in the research areas of semiconductor physics and organic photonics and might lead to a second revolution triggered by fluorescent proteins. The persistent seek for new emerging materials in optics and photonics has identified FPs in their solid state as promising bright and stable light emitters in photonic structures such as optical microcavities^{6,7}. Especially their spectral characteristics (self-absorption, optical gain etc.) have triggered extensive research in using FPs as active material for photon^{6,8} or polariton lasing experiments⁹. Those experiments revealed that microcavities filled with fluorescent protein show extremely low lasing thresholds and remarkable photostability compared to other fluorescent dyes⁹. Those advantages originate from the molecular structure of FPs, which is unique among organic dyes. The chromophore is basically surrounded by a protecting layer

of β -sheets, effectively forming a barrel (see Fig.1(a)). This barrel-like geometry ensures a strong reduction of concentration-induced luminescence quenching related to singlet-singlet annihilation and largely suppresses bimolecular quenching at high excitation densities⁹. It further maintains a fixed distance between neighboring chromophores in its solid state and thus supports efficient energy transfer between next neighbors⁶.

While fluorescent proteins and their exciton dynamics are well investigated in solution where chromophore concentrations are fairly small and inter-molecule distances are rather long, almost nothing is known about FPs in their solid state where chromophores are expected to be densely packed and inter-molecule interactions become highly relevant. Especially, the strength of light-matter interactions in microcavities between FP chromophores and photons (confined in the cavity) strongly depend on the timescales on which excitons decay. In this letter, we present a detailed investigation of the fundamental characteristics of Frenkel excitons (excitons localized at molecular sites; term chosen in analogy to solid state physics) in solid-state fluorescent proteins with respect to their potential use as active material in photonic applications. This includes inherent properties such as the identification of individual recombination centers, their lifetime as well as thermally activated decay processes. As model system we have chosen the green-emitting monomer eGFP (enhanced green fluorescent protein). Fluorescence measurements (time-resolved and time-binned) reveal a pronounced reduction of exciton lifetimes (when going from the solved phase to the solid state) due to concentration-induced self-quenching. We further identify a thermally-activated quenching process with an activation energy of 15 meV and a lifetime of 700 ps possibly related to conformational changes between protonated states.

Solid-state thin films of the fluorescent protein eGFP are prepared from highly concentrated protein solutions drop-casted on glass substrates. The proteins are expressed from *E.coli* bacteria (details about the protein

^{a)}Electronic mail: christof.dietrich@physik.uni-wuerzburg.de

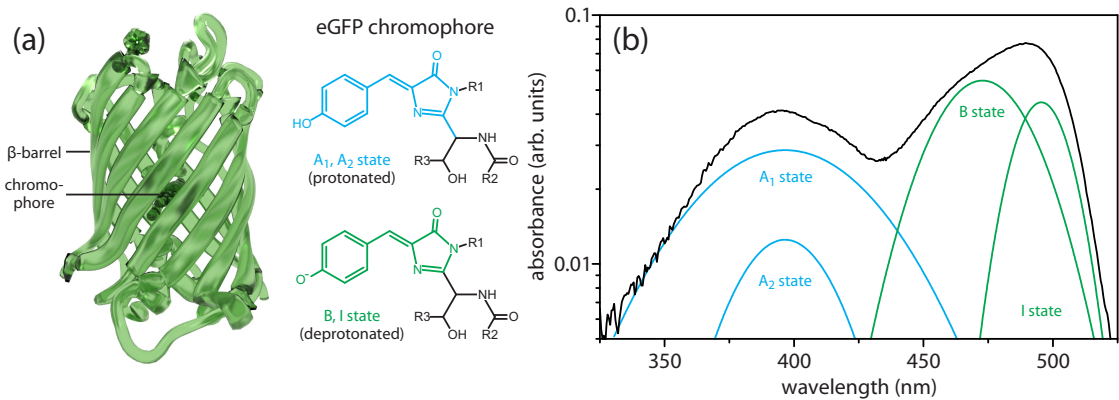


FIG. 1. (a) The molecular structure of enhanced green fluorescent protein (eGFP). The chromophore is surrounded by 11 β -sheets. By exciting the molecule with a pump laser wavelength below 420 nm, the chromophore occurs in its neutral (protonated) forms (A₁ and A₂ state) and its anionic (deprotonated) forms (B and I states). (b) Room-temperature absorption spectrum of eGFP with individual contributions from A, B and I states.

expression as well as the concentration procedure can be found in Ref.⁹) and initially solved in water. For fluorescence spectroscopic measurements, the respective thin films are pumped by a pulsed laser diode emitting at 375 nm with pulses of 50 ps length. The sample fluorescence is dispersed in a 500 mm spectrograph and detected using either a peltier-cooled charged coupled device (time-binned measurements) or an avalanche photodiode (time-resolved measurements, 400 ps temporal resolution). In the latter case, the spectrograph is utilized as spectral isolator of individual transitions (we have chosen an exit slit opening of 300 μ m that relates to a filter bandwidth of about 1 nm). Temperature-dependent fluorescence spectroscopy was performed in a helium flow cryostat.

Figure 1(b) shows the absorption spectrum of an eGFP thin film dried from solution. The overall absorption is composed of different absorption bands (the individual contributions were revealed by fitting the spectrum using a number of Gaussian peaks). In analogy to measurements on eGFP and (wild-type) wt-GFP in solution, we can identify contributions of individual bands and assign them to different molecular states¹⁰. The short-wavelength band can be assigned to absorption from molecules that are present in their neutral protonated shape (so-called A state). The A state absorption appears at 397 nm (3.12 eV). A state fluorescence is photo-activatable and only observable when the sample is excited by laser light with $\lambda_{\text{ex}} < 450$ nm¹². The other two absorption bands at longer wavelengths can be identified as contributions from anionic deprotonated chromophores that are distinguished by a relaxed (B state) and an unrelaxed (intermediate state) configuration. The latter (so-called I state) is partially created by an excited state proton transfer process (ESPT) from the A state configuration while no proton transfer is established between the protonated A state and deprotonated B state¹¹. For our solid-state eGFP samples, the B state

absorbs at 472 nm (2.63 eV) while the intermediate I state absorption lies at 496 nm (2.50 eV).

Note that we have included two degenerate A states (A₁ and A₂) of which one undergoes ESPT to the I state (A₁) and the other (A₂) is believed to undergo a conformational change into the A₁ state¹². The fluorescence spectrum of eGFP (see Fig.2(a)) is dominated by the radiative decay of both deprotonated states B and I at the same wavelength of 508 nm (2.44 eV) while the protonated A states weakly emit at 478 nm (2.59 eV). However, the A state emission only appears when the system is excited at a wavelength < 450 nm. The pronounced shoulder of the dominant fluorescent transition at longer wavelengths (at 540 nm) was earlier assigned to the radiative recombination of phonon replica of the B as well as the I state¹³.

In order to gain insight into the dynamic processes of Frenkel excitons in solid-state eGFP, we have subsequently recorded the time-resolved fluorescence of the three main recombination bands present in Fig.2(a). They can be seen in Fig.2(b). While all fluorescence bands decay on a ns-scale, the individual decay curves look different. The transitions at 508 nm and 540 nm decay mono-exponentially in good approximation (the 540-nm-band shows a slower turn-on-time due to the involvement of phonons), their decay times can be determined to be almost equal ($\tau(508 \text{ nm}) = \tau(540 \text{ nm}) = 2.45 \text{ ns}$). Note that those exciton lifetimes are notably shorter compared to similar investigations on eGFP in solution, where decay times of 3.1-3.4 ns are observed¹². We attribute this reduction to (concentration-induced) self-quenching by interactions between neighboring chromophores which are much more pronounced in the solid state than in solution.

For a more quantitative insight into the influence of the transition from the solved phase into the solid state on the radiative decay of eGFP transitions, we have performed time-resolved lifetime measurements at different

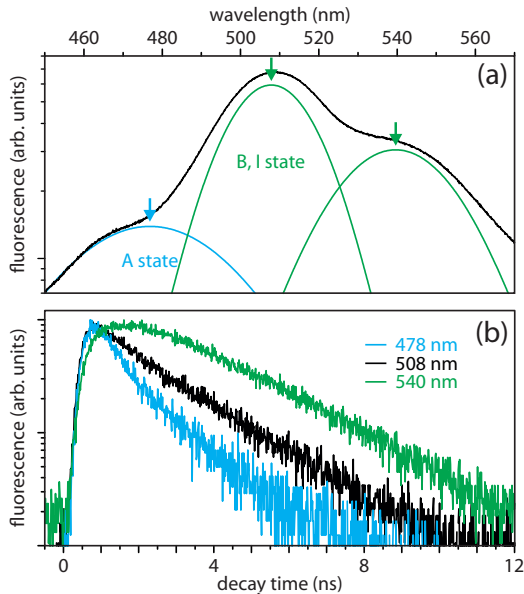


FIG. 2. (a) Fluorescence spectrum of solid-state eGFP. Individual Gaussian peaks reveal contributions of individual protein states. Inset: Schematic energy diagram of solid-state eGFP. (b) Time-resolved fluorescence decay recorded for three different wavelengths: 478 nm, 508 nm and 540 nm.

time intervals after dropcasting eGFP solved in water onto a glass substrate. The focal point of the microscope objective was adjusted to the interface between glass and eGFP and probed a constant volume during measurements. The recorded time-dependent evolution of the integrated (unfiltered) fluorescence intensity can be seen in Fig.3 (grey diamonds). The strong increase in fluorescence over time is a clear indication for the increase of eGFP molecule density and a strong reduction of the intermolecular distance as more and more chromophores contribute to the fluorescence in the probed sample region. This is a result of the vaporization process of the solvent and takes almost one week. Coincidentally, the exciton lifetime (blue circles in Fig.3) decreases from 3.05 ns (solution) to 2.45 ns (solid state) within the first week after drop-casting, after that it stays almost constant. The reduction of the exciton lifetime can be explained by two processes: on the one hand, a reduced inter-molecular distance increases the Förster resonance energy transfer (FRET) rate between neighboring chromophores (likewise enhancing energy transfer to molecules outside the detection area)⁶. On the other hand, densely packed chromophores are subject to fluorescence quenching caused by bi-molecular annihilation⁹. However, both processes reduce the exciton lifetime of proteins¹⁴. Note that the linewidth of the main emission bands does not narrow during the drying process from which we deduce a high degree of disorder in the solid state.

In contrast to the two main fluorescence bands, the transition at 478 nm (A state emission) does not decay

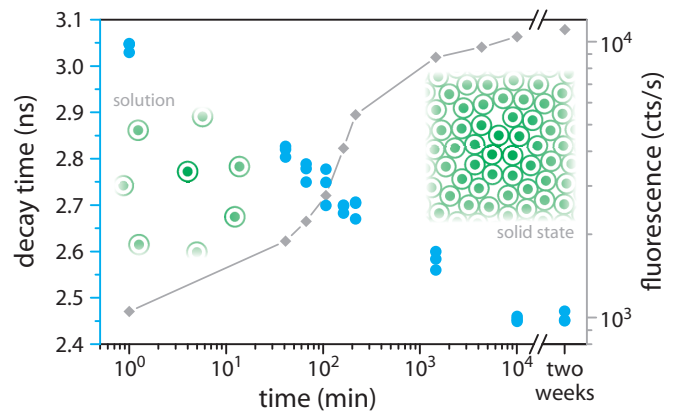


FIG. 3. Decay time of eGFP excitons determined from fits to the time-resolved fluorescence for different times after sample preparation (spectrally isolated at 542 nm to exclude contributions from the A state). Hereby, the first data point (at first minute) represents eGFP in its solved phase.

mono-exponentially at room temperature, but can well be fitted by a bi-exponential decay function. A fast decay with a time constant of only $\tau_1 = 0.7$ ns is followed by a slower decay with $\tau_2 = 2.4$ ns. Whereas the slower decay can be identified as the excited A state lifetime (and confirming an almost constant exciton lifetime for all excitonic configurations), the appearance of an additional fast initial decay has been observed before^{12,15,16} and was attributed to conformational changes of the protonated state induced by surrounding hydrogen¹². However, in contrast to earlier investigations on solutions ($\tau_1 = 0.25$ ns¹²), the determined time constant for the faster process in the solid state is considerably larger ($\tau_1 = 0.7$ ns). This is consistent since eGFP chromophores in the solid state are surrounded by other eGFP molecules rather than other chemical species. Thus, interactions with these species may be suppressed (explaining the increase in τ_1). This suggests that this fast decay might be related to intermolecular photophysical processes of the chromophore with its environment, e.g. through proton transfer.

The evolution of excited state dynamics can be tracked best by temperature-dependent measurements as those provide insight into the population of individual states as well as thermally activated kinetics. We have therefore placed the solid-state protein thin films into a cryostat and performed time-resolved and time-binned fluorescence spectroscopy on the A state emission in a temperature range between 10 and 300 K (decay curves for room and cryogenic temperatures are shown in Fig.4(a)). The determined decay times (from fits to the time-dependent decay curves) are shown in Fig.4(b). When decreasing the temperature from 300 K, we observe an increase of the exciton lifetime. This increase is most commonly attributed to the freeze-out of higher excited states with reduced lifetimes¹⁶. Apart from that, we further observe an increase in the turn-on time of the fluorescence signal

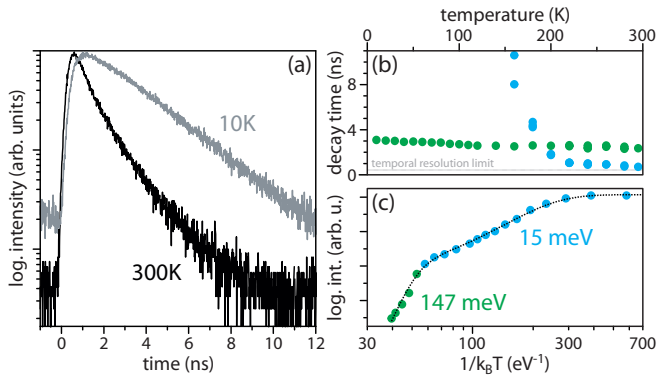


FIG. 4. (a) Time-resolved luminescence of the weak (A state) emission band at 478 nm recorded at cryogenic (gray line) and room temperature (black line). (b) Temperature-dependent decay times of the A state (τ_1 as blue and τ_2 as green dots, respectively) determined from bi-exponential ($T > 170$ K) respective mono-exponential fits (≤ 170 K) to the time-resolved luminescence. (c) The integrated A state eGFP fluorescence vs. inverse thermal energy. The dashed black line represents a Bose-Einstein fit accounting for two thermally activatable decay processes with activation energies of 15 meV (blue dots) and 147 meV (green dots).

(rise time of the emission) from 0.7 ns (at room temperature) to 1.1 ns (at 10 K), which we attribute to the depopulation of vibronic states at low temperatures effectively slowing down the relaxation from (energetically) higher excited states into the lowest-lying excited state.

While the increase of the exciton lifetime is steady over the investigated temperature range, the shorter decay time constant (τ_1) increases much faster with decreasing temperature and is effectively not resolvable anymore at temperatures below 170 K. Subsequently, the decay curves change to a strictly mono-exponential behavior (only caused by radiative decay of excitons, see Fig.4(a)). While at this stage, we cannot fully identify the origin of the shorter decay, we find this decay to be thermally activatable with a thermal activation energy of 15 meV (corresponding to an activation temperature of 170 K). This indicates that the shorter decay may involve the escape and re-capture of a proton. When lowering the temperature, the proton does not possess enough energy to escape. This interpretation is supported by the work of Fang *et al.*¹⁷, who observed a molecular vibration at 120 cm^{-1} (corresponding to about 15 meV) that facilitates the rearrangement of hydrogen bonds and thus enables proton transfer.

To confirm the presence of such a thermally activated process, we have further recorded the temperature-dependent (time-binned) fluorescence and fitted the spectra with a number of Gaussian peaks accounting for the protonated and deprotonated states as well as pronounced vibronic replica. The temperature-dependent integrated intensity of the A state emission band is shown in Fig.4(c), right, and reveals two distinct intensity

quenching processes in the temperature range of interest. A Bose-Einstein fit to the experimental data yields thermal activation energies of two processes of (147 ± 15) meV and (15 ± 1) meV. While the lower energy is in very good agreement with the energy determined for the shorter decay, the higher value can be attributed to the exciton binding energy of the A state excitons (the energy necessary to create free carriers).

In summary, we have investigated the exciton dynamics in solid-state enhanced green fluorescent protein. We have identified the contribution from protonated (A state) and deprotonated (B and I state) molecular configurations in both absorption and emission spectra characteristic for solid-state eGFP. The exciton lifetime for all excitonic complexes is almost equal and reduces from 3.05 ns in solution to 2.45 ns in the solid state, as a consequence of FRET and annihilation processes. Temperature-dependent fluorescence measurements further identify two thermally activated fluorescence quenching processes with activation energies of 147 meV and 15 meV. While the first process is assigned to the exciton binding energy of the eGFP chromophores, the latter is associated with a conformational change possibly facilitating proton transfer.

S.H. gratefully acknowledges support by the Engineering and Physical Sciences Research Council of UK through the "Hybrid Polaritonics" Program Grant (Project EP/M025330/1).

REFERENCES

- ¹J. Wiedenmann, H. Oswald, and U. Nienhaus, *IUBMB Life* 61, 1029-1042 (2009).
- ²M. Fernandez-Suarez and A.Y. Ting, *Nat. Rev. Mol. Cell Bio.* 9, 929-943 (2008).
- ³R.M. Hoffmann, *Lab. Invest.* 95, 432-452 (2015).
- ⁴M. Chalfie, Y. Tu, G. Euskirchen, W.W. Ward, and D.C. Prasher, *Science* 263, 802-805 (1994).
- ⁵M.C. Gather and S.H. Yun, *Nat. Photon.* 5, 406-410 (2011).
- ⁶M.C. Gather and S.H. Yun, *Nat. Comm.* 5, 5722 (2014).
- ⁷C.P. Dietrich, S. Höfling, and M.C. Gather, *Appl. Phys. Lett.* 105, 233702 (2014).
- ⁸H.J. Oh, M.C. Gather, J.-J. Song, and S.H. Yun, *Opt. Expr.* 22, 31411 (2014).
- ⁹C.P. Dietrich, A. Steude, L. Tropic, M. Schubert, N.M. Kronenberg, K. Ostermann, S. Höfling, and M.C. Gather, *Sci. Adv.* 2, e1600666 (2016).
- ¹⁰R. Heim, D.C. Prasher, and R.Y. Tsien, *Proc. Natl. Acad. Sci. USA* 91, 12501 (1994).
- ¹¹M. Chatteraj, B.A. King, G.U. Bublitz, S.G. Boxer, *Proc. Natl. Acad. Sci. USA* 93, 8362 (1996).
- ¹²M. Cotlet, J. Hofkens, M. Maus, T. Gensch, M. v.d. Auweraer, J. Michiels, G. Dirix, M. v. Guyse, J. Vanderleyen, A.J.W.G. Visser, and F.C. De Schryver, *J. Phys. Chem. B* 105, 4999 (2001).
- ¹³T.M.H. Creemers, A.J. Lock, V. Subramaniam, T.M. Jovin, and S. Völker, *Nat. Struct. Biol.* 6, 557-560 (1999).
- ¹⁴B. Valeur and M.N. Berberan-Santos, *Molecular Fluorescence* (Wiley-VCH, Weinheim, 2012).
- ¹⁵A. Volkmer, V. Subramaniam, D.J.S. Birch, and T.M. Jovin, *Biophys. J.* 78, 1589 (2000).
- ¹⁶P. Leiderman, R. Gepshtein, I. Tsimberov, and D. Huppert, *J. Phys. Chem. B* 112, 1232-1239 (2008).

